Hydrodynamics of Large Objects in the Sea Part I—Hydrodynamic Analysis

C. J. Garrison*
Naval Postgraduate School, Monterey, Calif.

This paper deals with the hydrodynamic forces exerted on a rigid object describing harmonic oscillations under or on a free surface as well as the forces resulting from the interaction of the object held fixed in a train of regular surface waves. The problem is formulated for a body of arbitrary shape in water of finite depth and the development of a numerical scheme for carrying out the calculations is described. An energy balance as well as Haskind's relations are used as a check on the accuracy of the numerical results. Numerical results are presented for a floating sphere, a vertical circular cylinder, and a practical semi-immersed caisson configuration.

Nomenclature

$\bar{a}$ = characteristic dimension of body
C_i = wave force (or moment) coefficient, Eqs. (36) and (40)
C_{ij} = ith component force (or moment) coefficient associated with the jth component motion
$\bar{d}$ = depth of submergence
$d\bar{S}$ = differential surface area
f = source strength function
G = Green's function
g = acceleration of Gravity
g_i = (i = 1,2,...7) See Eq. (19)
$\bar{h}$ = water depth
$\bar{H}$ = wave height
$\mathbf{i},\mathbf{j},\mathbf{k}$ = cartesian unit vectors
$\bar{L}$ = wavelength
M_{ij} = added mass coef., (added mass/$\rho\bar{a}^3$) or (added mom. of $I/\rho\bar{a}^5$)
N_{ij} = damping coef., (linear damping/$\rho\sigma\bar{a}^3$) or (angular damping/$\rho\sigma\bar{a}^5$)
$\mathbf{n}$ = unit outward normal vector
P' = pressure associated with diffraction of incident wave
P_j = (j = 1,2,...6) pressure associated with the 6 degrees of freedom
$\bar{\mathbf{q}}$ = fluid velocity vector
R_e = real part
t = time
T = wave period
u = dimensionless potential function
x,y,z = cartesian coordinates, dimensionless
$\bar{X}_i$ = body lineal displacement
$\bar{\eta}$ = elevation of free surface
Θ_i = body angular displacement
ν = $\sigma^2\bar{a}/g$, frequency parameter
ξ,η,ζ = point on body
ρ = fluid density
σ = frequency, $2\pi/T$
ϕ_0 = incident wave potential
ϕ_7 = scattering potential
ϕ_i = (i = 1,2,...6) potential associated with 6 degrees of freedom
δ = dirac delta function
δ_{ij},δ_i = phase shift angles

Introduction

THE pressure distribution and resulting hydrodynamic forces exerted on rigid objects immersed in water in the presence of a free surface is a problem of interest to naval architects as well as ocean engineers. In the design of large submerged or semisubmerged structures such as offshore drilling rigs or submerged oil storage tanks, the forces exerted by surface waves are important considerations. In the mooring of vessels at sea, for example, both the forces induced by surface waves as well as the forces induced by the dynamic response of the vessel are important factors in the determination of the resulting motion. The former quantities are generally referred to as simply wave forces or excitation forces while the latter are often characterized by an added mass and damping coefficient.

The present paper deals with the hydrodynamic aspect of such problems. Essentially, two different types of fluid motion are considered, namely, the interaction of a train of regular surface waves with the rigid object, and the fluid motion produced by the harmonic oscillation of the object in otherwise still water. While these two problems are physically distinct, they are mathematically similar and as a result are dealt with simultaneously herein.

When dealing with unsteady flow about immersed bodies, it is generally understood that a potential (or inviscid) flow analysis is a valid approximation to the real flow, provided the amplitude of the motion is sufficiently small. For example, in the case of unidirectional flow with constant acceleration past circular cylinders, Sarpkaya and Garrison[1] found that at the beginning of the motion the flow was unseparated, and accordingly, the added mass coefficient was equal to its potential value of 1.0 while the drag coefficient was zero. Keulegan and Carpenter[2] found similar behavior for the case of oscillatory flow past circular cylinders and plates. Thus, if the amplitude of the fluid motion is sufficiently small, it may be expected that inviscid flow assumptions as applied herein should yield valid results. It is understood, therefore, that the wave amplitude or amplitude of body motion is assumed to be small compared to the characteristic dimensions of the object.

Forces exerted on cylinders floating at the free surface both held fixed in regular waves as well as describing harmonic oscillations have been the subject of a number of papers. Examples are the work of Dean and Ursell,[3] Porter,[4] Vugts,[5] and Kim.[6] Similar work on three dimensional objects is, however, much more limited. Kim[6] presented added mass and damping coefficients for a semi-ellipsoidal body with its origin on the free surface in water of infinite depth and Garrison and Seetharama Rao[7] presented both theoretical and experimental results for wave forces acting on a hemisphere with its center on the bottom. Recently, Milgram and Halkyard[8] presented results for the oscillation of an axisymmetric bulbous body and a sphere in still water of infinite depth. Garrison and Chow[9] have compared theoretical and experimental results for the wave forces acting on a practical submerged oil storage tank configuration.

The present paper deals with three-dimensional objects of arbitrary shape in water of finite depth. The theory and numerical procedure is developed with the end toward the practical numerical calculations for arbitrary shapes of practical utility. Numerical results are presented for the

Received March 30, 1973; revision received September 6, 1973.
Index categories: Hydrodynamics; Marine Vessel Design.
*Associate Professor, Department of Mechanical Engineering.

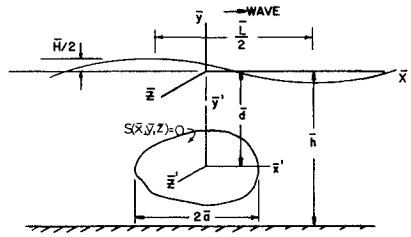

Fig. 1 Definition schematic.

wave force problem where the object is held fixed in a train of surface waves as well as for the case where the body undergoes harmonic oscillations in otherwise still water. Computations were made for a vertical circular cylinder and a floating hemisphere, and a method for checking the convergence of the numerical scheme is proposed. Numerical results are also presented for a bottom-mounted ocean caisson of practical configuration.

Formulation of the Problem

Consider a rigid object of arbitrary shape and having characteristic lineal dimension $\bar{a}$ submerged to a depth $\bar{d}$ beneath the free surface in water of depth $\bar{h}$ as shown in Fig. 1. The body is considered to be smooth to the extent that its unit normal vector is a continuous function and it may or may not intersect the free surface or bottom. Two coordinate systems are identified, $\bar{x},\bar{y},\bar{z}$ coordinates with origin fixed at the free surface and the body coordinates $\bar{x}',\bar{y}',\bar{z}'$ located at depth $\bar{y} = -\bar{d}$. The bars over the symbols denote dimensional quantities.

The problem set forth herein deals with the fluid motion and forces induced by the small amplitude oscillation of the object in its 6 degrees of freedom as well as the fluid motion associated with the interaction of the fixed object with a train of regular waves. The small amplitude oscillatory motion of the object about its equilibrium position with frequency σ is described by the relationships,

$$\bar{X}_j(t) = \bar{X}_j^0 Re[e^{-i\sigma t}], \quad j = 1,2,3 \tag{1a}$$

$$\Theta_j(t) = \Theta_j^0 Re[e^{-i\sigma t}], \quad j = 4,5,6 \tag{1b}$$

where the subscript $j = 1,2,3$ denotes oscillation in the $\bar{x}'$,-$\bar{y}'$,$\bar{z}'$ directions, respectively, and $j = 4,5,6$ denotes angular oscillation about the $\bar{x}'$,$\bar{y}'$,$\bar{z}'$ axes, respectively. The real numbers $\bar{X}_j^0$ and θ_j^0 denote the amplitudes of the motion. In the case of ship motion $\bar{X}_1$,$\bar{X}_2$ and $\bar{X}_3$ are referred to as surge, heave and sway while the angular components Θ_4, Θ_5, and Θ_6 are called roll, yaw, and pitch, respectively. The second problem considered here is the interaction of a train of regular surface waves with the object fixed in space. The regular incident waves of wave height $2\bar{\eta}^0 = \bar{H}$ and wavelength $\bar{L}$ are assumed to progress in the positive x-direction.

The fluid is assumed to be incompressible, and the motion irrotational and harmonic with time dependence $e^{-i\sigma t}$ in all cases. It follows, therefore, that a velocity potential exists such that the fluid velocity vector may be defined as

$$\bar{q}_j = Re[\bar{\nabla}\phi_j e^{-i\sigma t}], \quad j = 1,2,..6 \tag{2}$$

where ϕ_j denotes the velocity potential associated with the motion induced by oscillations in the 6 degrees of freedom and $\bar{\nabla} = \mathbf{i}(\partial/\partial\bar{x}) + \mathbf{j}(\partial/\partial\bar{y}) + \mathbf{k}(\partial/\partial\bar{z})$, $\mathbf{i},\mathbf{j},\mathbf{k}$ being the unit vectors in the $\bar{x},\bar{y},\bar{z}$ directions, respectively. In the case of regular wave interaction with the fixed object the velocity potential may be written as the sum

$$\phi' = \phi_0 + \phi_7 \tag{3}$$

where ϕ_0 denotes the velocity potential of the incident wave in the absence of the object and ϕ_7 denotes the velocity potential of the scattered wave due to the presence of the rigid object. For this case, the fluid velocity vector is given by

$$\bar{q}' = Re[\bar{\nabla}(\phi_0 + \phi_7)e^{-i\sigma t}] \tag{4}$$

Continuity considerations implies that ϕ_j, ($j = 0,1,2, \ldots .$ 7) must satisfy the Laplace equation

$$\bar{\nabla}^2\phi_j = 0 \tag{5}$$

and from the linearized form of Bernoulli's equation, which is applied throughout, the dynamic fluid pressure is given by

$$P_j = Re[i\rho\sigma\phi_j e^{-i\sigma t}], \quad j = 1,2,\ldots 6 \tag{6}$$

For the second problem, involving wave interaction with the fixed object, the pressure is given by

$$P' = Re[i\rho\sigma(\phi_0 + \phi_7)e^{-i\sigma t}] \tag{7}$$

The velocity potential must satisfy certain boundary conditions in addition to Eq. (5). These include the linearized free surface boundary condition

$$\frac{\partial\phi_i}{\partial\bar{y}}(\bar{x},0,\bar{z}) - \frac{\sigma^2}{g}\phi_i(\bar{x},0,\bar{z}) = 0, \quad i = 0,1,2,\ldots .7 \tag{8}$$

as well as the kinematic boundary condition on the bottom

$$\frac{\partial\phi_i}{\partial\bar{y}}(\bar{x},-\bar{h},\bar{z}) = 0, \quad i = 0,1,2,\ldots 7 \tag{9}$$

The surface of the object in its mean position is described by

$$S(\bar{x},\bar{y},\bar{z}) = 0 \tag{10}$$

and the kinematic boundary conditions on this surface are given by

$$\frac{\partial\phi_1}{\partial\bar{n}} = -i\sigma\bar{X}_1^0 n_x \tag{11a}$$

$$\frac{\partial\phi_2}{\partial\bar{n}} = -i\sigma\bar{X}_2^0 n_y \tag{11b}$$

$$\frac{\partial\phi_3}{\partial\bar{n}} = -i\sigma\bar{X}_3^0 n_z \tag{11c}$$

$$\frac{\partial\phi_4}{\partial\bar{n}} = -i\sigma\Theta_4^0[(\bar{d} + \bar{y})n_z - \bar{z}n_z] \tag{11d}$$

$$\frac{\partial\phi_5}{\partial\bar{n}} = -i\sigma\Theta_5^0[\bar{z}n_x - \bar{x}n_z] \tag{11e}$$

$$\frac{\partial\phi_6}{\partial\bar{n}} = -i\sigma\Theta_6^0[\bar{x}n_y - (\bar{d} + \bar{y})n_x] \tag{11f}$$

$$\frac{\partial\phi_7}{\partial\bar{n}} = -\frac{\partial\phi_0}{\partial\bar{n}} \tag{11g}$$

where $\mathbf{n} = \mathbf{i}n_x + \mathbf{j}n_y + \mathbf{k}n_z$ denotes the unit normal vector on the surface of the object directed outward into the fluid and $\bar{d}$ denotes the depth of submergence of the $\bar{x}'$,$\bar{y}'$,$\bar{z}'$, coordinate origin. Finally, the velocity potential ϕ_i must satisfy the radiation condition which allows only outgoing waves,

$$\phi_i(\bar{r},\theta,\bar{y}) - \lambda_i(\theta)\bar{r}^{-1/2}\frac{\cosh[k(\bar{y}+\bar{h})]}{\cosh(k\bar{h})}e^{ik\bar{r}_1} \to 0, \bar{r}, \to \infty \tag{12}$$

where $\bar{r}_1 = [\bar{x}^2 + \bar{z}^2]^{1/2}$ and $\theta = \tan^{-1}(\bar{z}/\bar{x})$. The wave number is defined as $k = 2\pi/\bar{L}$ where $\bar{L}$ denotes the wave length and is related to the frequency of the disturbance according to the well known relationship

$$\frac{\sigma^2}{g} = k\tanh(k\bar{h}) \tag{13}$$

The velocity potential of the incident wave alone progressing in the positive $\bar{x}$-direction is given by

$$\phi_0(\bar{x},\bar{y}) = -\frac{ig\bar{\eta}^0}{\sigma}\frac{\cosh[k(\bar{h}+\bar{y})]}{\cosh(k\bar{h})}e^{ik\bar{x}} \tag{14}$$

where $\bar{\eta}^0 = \bar{H}/2$ denotes the amplitude of the incident wave, $\bar{H}$ being the wave height.

For convenience in carrying out the solution for ϕ_i and to show clearly the dependence of the solution on the parameter, $a = 2\pi\bar{a}/\bar{L} = k\bar{a}$, the relative water depth, $h = \bar{h}/\bar{a}$, and the relative depth of submergence, $d = \bar{d}/\bar{a}$, we shall first make the space variables and amplitudes dimensionless with the characteristic linear dimension of the object,

$$x = \bar{x}/\bar{a},\ y = \bar{y}/\bar{a},\ z = \bar{z}/\bar{a},\ r = \bar{r}/\bar{a}$$
$$X_i^0 = X_i^0/a,\ (i = 1,2,3);\ X_i^0 = \Theta_i^0,\ (i = 4,5,6)$$
$$\eta^0 = \bar{\eta}^0/\bar{a} = \bar{H}/2\bar{a}$$

and then introduce the dimensionless potential functions, u_j, as

$$\begin{aligned} i\sigma\phi_j(\bar{x},\bar{y},\bar{z})/g\bar{a}X_j^0 &= a\tanh(ah)\,u_j(x,y,z),\ j = 1,2,\ldots 6 \\ i\sigma\phi_7(\bar{x},\bar{y},\bar{z})/g\bar{a}\eta^0 &= -a\,u_7(x,y,z) \\ i\sigma\phi_0(\bar{x},\bar{y})/g\bar{a}\eta^0 &= -a\,u_0(x,y) \end{aligned} \tag{15}$$

The complex dimensionless dynamic pressure amplitude can now be written by use of the linearized form of Bernouli's equation, (6) and (7)

$$\begin{aligned} p_j &= a\tanh(ah)\,u_j(x,y,z),\ j = 1,2,\ldots 6 \\ p' &= \frac{\cosh[a(h+y)]}{\cosh(ah)}e^{iax} - a\,u_7(x,y,z) \end{aligned} \tag{16}$$

where the complex amplitude of the pressure p is defined as

$$\begin{aligned} \frac{P_j}{\rho g\bar{a}X_j^0} &= Re[p_j e^{-i\sigma t}],\ j = 1,2,\ldots 6 \\ \frac{P'}{\rho g\bar{a}\eta^0} &= Re[p' e^{-i\sigma t}] \end{aligned} \tag{17}$$

The boundary value problem which describes the fluid motion arising from the oscillation of the rigid object in its 6 degrees of freedom as well as the scattering of the incident wave may now be written concisely in terms of dimensionless parameters. The potentials $u_i(x,y,z)$, $i = 1,2,\ldots 7$, continuous in the fluid region is sought such that

$$\nabla^2 u_j(x,y,z) = 0,\ (\text{outside } S(x,y,z) = 0) \tag{18a}$$

$$\frac{\partial u_j}{\partial y}(x,0,z) - a\tanh(ah)\,u_j(x,0,z) = 0 \tag{18b}$$

$$\frac{\partial u_j}{\partial y}(x,-h,z) = 0 \tag{18c}$$

$$\frac{\partial u_j}{\partial n}(x,y,z) = g_j(x,y,z) \text{ on } S(x,y,z) = 0 \tag{18d}$$

$$u_j(r,\theta,y) - \lambda_j(\theta)\,r_1^{-1/2}\frac{\cosh[a(h+y)]}{\cosh(ah)}e^{iar_1} \to 0,\ r_1, \to \infty \tag{18e}$$

where g_j denotes the prescribed function which depends on the mode of oscillation ($j = 1,2,\ldots 6$), the subscript 7 corresponding to the scattering with g_7 being obtained from Eq. (14). These functions are

$$g_1 = n_x,\ g_2 = n_y,\ g_3 = n_z$$
$$g_4 = (d+y)n_z - zn_y,\ g_5 = zn_x - xn_z,\ g_6 = xn_y - (d+y)n_x$$
$$g_7 = \frac{1}{\cosh(ah)}\Big[n_y\sinh[a(h+y)] + in_x\cosh[a(h+y)]\Big]e^{iax} \tag{19}$$

Representation of the Potential

The potential function u_j may be represented by use of a Green's function having the physical interpretation of a point wave source of unit strength. These sources are distributed over the surface of the object according to the source strength function, f, so that the potential at some point (x,y,z) within the fluid is given by the surface integral

$$u_j(x,y,z) = \frac{1}{4\pi}\iint_S f_j(\xi,\eta,\zeta)\,G(x,y,z;\xi,\eta,\zeta)ds \tag{20}$$

where (ξ,η,ζ) represents a point on the surface of the object, G denotes the Green's function and $dS = d\bar{S}/\bar{a}$ denote the dimensionless surface area element. The Green's function is defined, therefore, as the function which satisfies

$$\nabla^2 G(x,y,z;\xi,\eta,\zeta) = \delta(x-\xi)\,\delta(y-\eta)\,\delta(z-\zeta) \tag{21}$$

as well as the boundary conditions (18b, c, e). Such a function is given by Wehausen and Laitone[10] as

$$G(x,y,z;\xi,\eta,\zeta) = \frac{1}{R} + G^* \tag{22}$$

where

$$G^*(x,y,z;\xi,\eta,\zeta) = \frac{1}{R'} + 2P.V.\int_0^\infty \frac{(\mu+\nu)e^{-\mu h}\cosh[\mu(\eta+h)]\cosh[\mu(y+h)]}{\mu\sinh(\mu h) - \nu\cosh(\mu h)}J_0(\mu r)d\mu \tag{23}$$

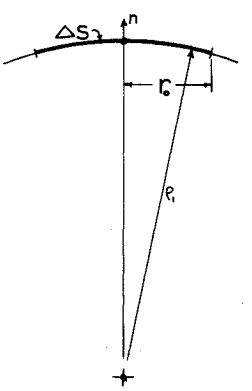

Fig. 2 Singular point.

$$+ i\,\frac{2\pi(a^2-\nu^2)\cosh[a(\eta+h)]\cosh[a(y+h)]J_0(ar)}{a^2h-\nu^2h+\nu}$$

$$R = [(x-\xi)^2+(y-\eta)^2+(z-\zeta)^2]^{1/2}$$

$$R' = [(x-\xi)^2+(y+2h+\eta)^2+(z-\zeta)^2]^{1/2}$$

$$r = [(x-\xi)^2+(z-\zeta)^2]^{1/2}$$

$$\nu = \frac{\sigma^2\bar{a}}{g} = a\tanh(ah)$$

and *P.V.* indicates principal value of the integral. An alternate series form of the Green's function is also given by Wehausen and Laitone[10] as

$$G(x,y,z;\xi,\eta,\zeta) = \frac{2\pi(\nu^2-a^2)}{a^2h-\nu^2h+\nu}\cosh[a(y+h)]\cosh[a(\eta+h)][Y_0(ar)-iJ_0(ar)] + 4\sum_{k=1}^{\infty}\frac{(\mu_k^2+\nu^2)}{\mu_k^2h+\nu^2h-\nu}\cos[\mu_k(y+h)]\cos[\mu_k(\eta+h)]K_0(\mu_k r) \quad (24)$$

where J_0 and Y_0 denote, respectively, Bessel functions of the first and second kind of order zero and K_0 denotes the modified Bessel function of the second kind of order zero. The quantities μ_k are the real positive roots of the equation

$$\mu_k\tan(\mu_k h)+\nu = 0 \quad (25)$$

The solution to the boundary value problem stated in Eq. (18) now rests on the determination of the source strength function f. Taking the normal derivative of the potential u_i and applying the boundary condition (18d) yields the following integral equation from which f is to be determined:

$$\frac{1}{4\pi}\iint_S f_j(\xi,\eta,\zeta)\frac{\partial G}{\partial n}(x,y,z;\xi,\eta,\zeta)dS = g_j(x,y,z),\ j = 1,2,\ldots 7 \quad (26)$$

where $\partial G/\partial n$ may be obtained by straightforward differentiation of Eqs. (23) or (24).

Numerical Solution

The integral equation (26) may be solved numerically beginning with the partitioning of the surface of the object into N area elements of size ΔS_i where the subscript takes on values $i = 1,2,3 \ldots N$. Since the source strength function, f, occurring in the integrals in Eqs. (20) and (26), is a continuous, well-behaved function, these integrals may be approximated by the following summations:

$$f_{n_j}\alpha_{ij} = g_{n_i} \quad (27)$$

$$u_{n_i} = f_{n_j}\beta_{ij} \quad (28)$$

where

$$\alpha_{ij} = \frac{1}{4\pi}\iint_{\Delta S_j}\frac{\partial G}{\partial n}(x_i,y_i,z_i;\xi,\eta,\zeta)dS \quad (29)$$

$$\beta_{ij} = \frac{1}{4\pi}\iint_{\Delta S_j}G(x_i,y_i,z_i;\xi,\eta,\zeta)dS \quad (30)$$

In these expressions, u_{ni} denotes the potential at the ith nodal point on the object associated with either the nth mode of oscillation, or scattering ($n = 7$) of the incident wave. The integrations are to be carried out over the finite surface area elements ΔS_j and f_{nj} denotes the value of f_n at the central point of the area element. The approximation made here is consistent in that as N approaches infinity the approximations given in Eqs. (27) and (28) approach the exact forms.

Once the matrices α, β, and g are numerically evaluated, Eq. (27) may be easily inverted by use of a standard computer subroutine to obtain the solution for f_n. Using this information, u_n may then be easily obtained from Eq. (28). However, there are certain difficulties connected with the evaluation of Eqs. (29) and (30) which are noteworthy.

One such difficulty in the evaluation of α and β occurs for the special case where $i = j$. Although G^* and $\partial G^*/\partial n$ are everywhere regular, the $1/R$ and $\partial(1/R)/\partial n$ terms occurring in Eqs. (29) and (30) are singular as $R \to 0$ and, therefore, special consideration must be given to this case. Carrying out the integrations analytically for these two terms for an area element of rather general curvature is difficult, but it is possible to affect an analytical evaluation for a circular area element if the surface has constant curvature. Using the geometry indicated in Fig. 2, we may evaluate the following integrals analytically as

$$\iint_{\Delta S}\frac{1}{R}dS = 2\pi r_0 \quad (31)$$

$$\iint_{\Delta S}\frac{\partial}{\partial n}\left(\frac{1}{R}\right)dS = -2\pi\left(1-\frac{1}{2}\frac{r_0}{\rho_1}+\ldots\right) \quad (32)$$

For the special case considered, the integral of $1/R$ is independent of the curvature while the integral of $\partial/\partial n(1/R)$ involves the ratio of the radius of the element to radius of curvature, ρ_1, to the first power. Thus, if the curved area elements ΔS are taken as plane areas or small facets, for purposes of numerical calculation, an error of the order r_0/ρ_1 may be expected to result. Consequently, in order to keep this error to a minimum, the subdivision size is reduced in regions of sharp curvature of the immersed surface.

Although the result Eq. (31) is independent of the curvature, it is dependent on the shape of ΔS, and since rectangular elements, as opposed to circular, are a natural result when partitioning most shapes, it is instructive to evaluate the integral indicated in Eq. (31) for a plane rectangular area. The analytical integration of $(1/R)$ over a rectangle is straightforward, albeit algebraically involved, giving the result

$$\iint_{\Delta S}\frac{1}{R}dS = 2(\Delta S/b)^{1/2}\left\{\ln[b+(b^2+1)^{1/2}] + b\ln\left[\frac{1+(b^2+1)^{1/2}}{b}\right]\right\} \quad (33)$$

where b denotes the aspect ratio of the rectangular element, i.e., the width to length ratio. In order to demonstrate the effect of the rectangular, as opposed to a circular area, the factor representing the ratio of Eq. (33) to Eq. (31) is plotted in Fig. 3. It may be noted from the figure that the ratio is nearly unity for $b = 1$. showing that a square area element gives only a slightly different value than a circular area of equal size. However, at larger aspect ratios the effect becomes more pronounced, and the shape correction factor becomes necessary.

A second difficulty arises in the numerical evaluation of Eqs. (29) and (30) on account of the singular nature of the factor $[1/(\mu\tanh\mu h - a\tanh ah)]$ at $\mu = a$ which occurs in the infinite integral in Eq. (23) and its normal derivative. However, it can easily be shown that this factor is singular like $1/(\mu - a)$ and, therefore, the integral exists and can be numerically evaluated. For purposes of developing a digital computer program for the numerical inte-

gration in Eq. (23), a scheme similar to that used by Monacella[11] to integrate around the singularity was employed for the region $0 \lesssim \mu \lesssim 2a$ and, therefore, will not be discussed further here.

A sizable portion of the total computation time involved in the present problem is devoted to the numerical evaluation of the matrices (29) and (30). For this reason two different computer subroutines were utilized, one calculated G and $\partial G/\partial n$ based on the form given in Eqs. (22) and (23) while a second subroutine made the evaluations on the basis of the alternate series formulation given in Eq. (24). For elements of the α and β matrices corresponding to small values of (ar) the subroutine based on Eqs. (22) and (23) was utilized, while for larger values of (ar) the series form Eq. (24) was used because it converges rather rapidly and was found to require much less computer time than the integral form.

Hydrodynamic Forces and Moments

The forces and moments caused by the dynamic fluid pressure acting upon the immersed surface of the object may be obtained from the integrals

$$F_{ij}(t) = -(1 \text{ or } \bar{a}) \iint_S P_j g_i d\bar{S}, \quad i,j = 1,2,\ldots 6 \quad (34)$$

$$F_i(t) = -(1 \text{ or } \bar{a}) \iint_S P' g_i d\bar{S}, \quad i = 1,2,\ldots 6 \quad (35)$$

where F_i denotes the ith component of wave force (or moment) and F_{ij} denotes the ith component of forces arising from the jth component of body motion. The coefficient 1 is to be used in the case of a force ($i = 1,2,3$) while $\bar{a}$ is to be used when F denotes a moment ($i = 4,5,6$).

For purposes of presentation of the numerical results, dimensionless force coefficients are defined as

$$C_i = \frac{F_{i(\max)} e^{i\delta_i}}{\rho g \bar{a}^3 \eta^0}, \quad i = 1,2,3 \quad (36)$$

and

$$C_{ij} = \frac{F_{ij(\max)} e^{i\delta_{ij}}}{\rho \sigma^2 \bar{a}^4 X_j^0} = -M_{ij} - iN_{ij}, \quad \begin{matrix} i = 1,2,3 \\ j = 1,2,\ldots 6 \end{matrix} \quad (37)$$

The corresponding expressions for the moment coefficient are

$$C_i = \frac{F_{i(\max)} e^{i\delta_i}}{\rho g \bar{a}^4 \eta^0}, \quad i = 4,5,6 \quad (38)$$

and

$$C_{ij} = \frac{F_{ij(\max)} e^{i\delta_{ij}}}{\rho \sigma^2 \bar{a}^5 X_j^0} = -M_{ij} - iN_{ij}, \quad \begin{matrix} i = 4,5,6 \\ j = 1,2,\ldots 6 \end{matrix} \quad (39)$$

The complex coefficients C_i relate to the ith component of wave force (or moment) coefficient while C_{ij} denotes the ith component force (or moment) coefficient associated with the jth component of oscillation of the object. The phase shift angles δ_i and δ_{ij} relate the phase of the force to the crest of the incident wave and displacement of the body, respectively. The real and imaginary parts of the dimensionless force coefficients, M_{ij} and N_{ij}, are called the added mass and damping coefficient, respectively.

Using Eqs. (34) and (35) along with Eqs. (16) and (17) and the definitions Eqs. (36–39) the force coefficients may be written in dimensionless form as

$$C_i = \iint_S \left[au_7(x,y,z) - \frac{\cosh[a(h+y)]}{\cosh(ah)} e^{iax} \right] g_i(x,y,z) dS, \quad i = 1,2,\ldots 6 \quad (40)$$

and

$$C_{ij} = \iint_S u_j(x,y,z) g_i(x,y,z) dS, \quad i,j = 1,2,\ldots 6 \quad (41)$$

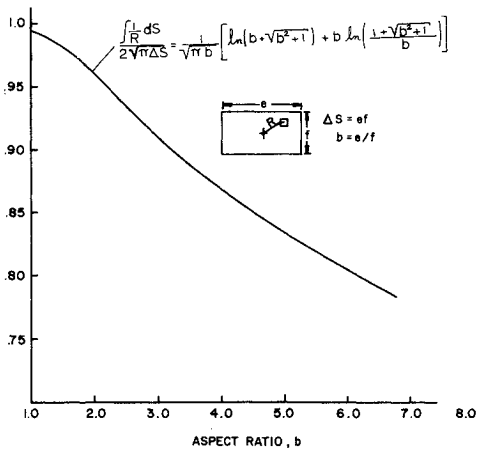

Fig. 3 Aspect ratio correction factor

Once $u_j(x,y,z)$ is obtained from Eq. (28) the coefficients may be obtained from Eqs. (40) and (41). For actual numerical evaluation the integrals in Eqs. (40) and (41) are replaced by summations.

Haskinds Relations and Energy Balance

Even though it may be supposed that the numerical solution proposed here will converge upon increasing the number of partitions, it is important to keep the partition size as large (and number of partitions as small) as accuracy considerations will permit in order to reduce computer time and storage requirements. It is, for this reason, important to determine the effect of the partition size on accuracy so that practical limits may be established.

One method of verifying the accuracy is to compare the numerical results with analytical results where closed form solutions exist. Although valid, this approach is limited to a few simple shapes; for more general shapes no such check, of course, exists.

A second method of checking the validity of the numerical results involves the use of an energy balance as well as the use of the so-called Haskinds relations. Conservation of energy requires that a balance must exist between the energy required to oscillate the object, and the wave energy transmitted across some control volume surrounding the object but at a large radial distance. Using the asymptotic form of the Green's function given in Eq. (24) along with Eq. (20) the following relationship for the damping coefficient is so obtained

$$N_{ii} = \frac{1}{4\pi} \left[\frac{a^2 - \nu^2}{h(a^2 - \nu^2) + \nu} \right] \int_0^{2\pi} \left| \iint_S f_i(\xi,\eta,\zeta) \cosh[a(\eta + h)] e^{-ia\gamma \cos(\beta - \theta)} dS \right|^2 d\theta \quad (42)$$

where $\gamma = (\xi^2 + \zeta^2)^{1/2}$ and $\beta = \tan^{-1}(\zeta/\xi)$. This relationship expresses the damping coefficient in terms of the far field behavior of the solution.

A relationship somewhat similar to Eq. (42) known as Haskind's relations, may be obtained for the wave force (or moment) coefficient. That is, the ith component wave force (or moment) coefficient is related to the waves produced at infinity by the body oscillating in the ith mode such that

$$C_i = \frac{1}{\cosh(ah)} \iint_S f_i(\xi,\eta,\zeta) \cosh[a(\eta + h)] e^{-ia\gamma \cos(\beta - \pi)} ds \quad (43)$$

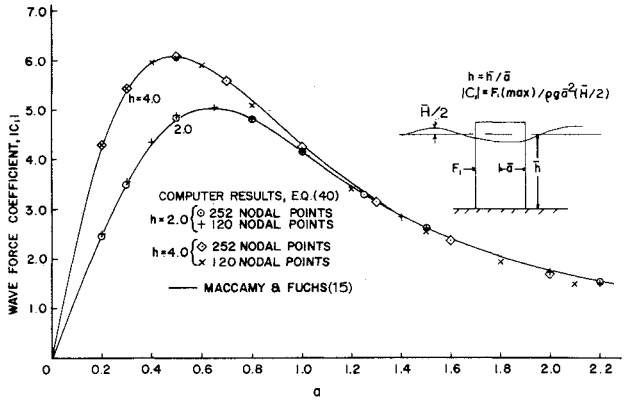

Fig. 4 Horizontal wave force coefficient for a vertical circular cylinder.

A form of this relationship between the wave force and the waves produced at infinity by the same body oscillating in otherwise still water was first derived by Haskind[12] and later reiterated and discussed by Newman.[13] Equation (43) may be considered to represent a form of the Haskind's relations as extended to the finite depth case. The details of this extension which involves integration by method of stationary phase are given by Seetharama Rao.[14]

Equations (42) and (43) represent relationships for the damping and wave force (or moment) coefficient based on the behavior of the far field solution. A comparison of these results with N_{ij} and C_i obtained from an integration of the pressure over the immersed surface, i.e., as obtained from Eqs. (40 and (41), provides a convenient and valuable self-check on the accuracy of numerical results. These results are not limited to special configurations and may be applied to arbitrary shapes. Equation (43) is, however, limited to symmetry with respect to the x-y plane, a condition which is satisfied by most practical shapes.

It may be noted, moreover, that for the case of the vertical force on an axisymmetric body a very simple relationship between the C_2 and N_{22} may be obtained from Eqs. (42) and (43). That is, in view of the axisymmetry the integrand in Eq. (42) must be independent of θ. Accordingly, the integration with θ may be accomplished by evaluating the integrand at any value of θ, say $\theta = \pi$ and multiplying by 2π. The right hand sides of Eqs. (42) and (43) then become similar and the following relationship may be derived between the wave force and damping coefficient in heave:

$$N_{22} = \frac{a}{2}\,\frac{\sinh(2ah)}{2ah + \sinh(2ah)}\,|C_2|^2 \tag{44}$$

For the case of infinite depth, Eq. (44) reduces to the special case presented by Newman[13]

$$|C_2| = \left(\frac{2\,N_{22}}{a}\right)^{1/2} \tag{45}$$

Discussion of Results

Numerical results have been generated for certain geometric configurations for purposes of comparison with corresponding closed form results of others and for purposes of studying the effects of the subdivision size on the accuracy of the numerical scheme. Also, rather extensive results are presented in order to show the effect of water depth on the hydrodynamic forces on a floating hemisphere.

The horizontal wave force coefficient is plotted in Fig. 4 for the case of a vertical circular cylinder extending between the bottom and free surface. MacCamy and Fuch's[15] corresponding closed form solution is also presented for comparison with the computer results and generally the agreement is excellent. For the $h = 2$ case very little difference exists between the results generated using 120 or 252 effective subdivisions. The results corresponding to the $h = 4$ case show a slightly greater spread between the computations based on 120 and 252 subdivisions. In either case the greatest error occurs at the largest value of the wavelength parameter, $a = 2\pi\bar{a}/\bar{L}$.

The results presented in Fig. 4 were obtained from Eq. (40) which results from an integration of the pressure over the immersed surface. A second method of evaluation of C_i based on the farfield results associated with the oscillation of the cylinder in surge is also possible. This result as given by Eq. (43) was also used to evaluate C_1 and the two results based on Eqs. (40) and (43) are compared in Fig. 5. The error plotted in Fig. 5 generally agrees with the trend of the errors indicated in Fig. 4. In the case of the cylinder of height $h = 2$ little difference between the results based on 120 and 252 subdivisions is evident and both results agree well with MacCamy and Fuch's closed form solution. This conclusion may also be deduced from

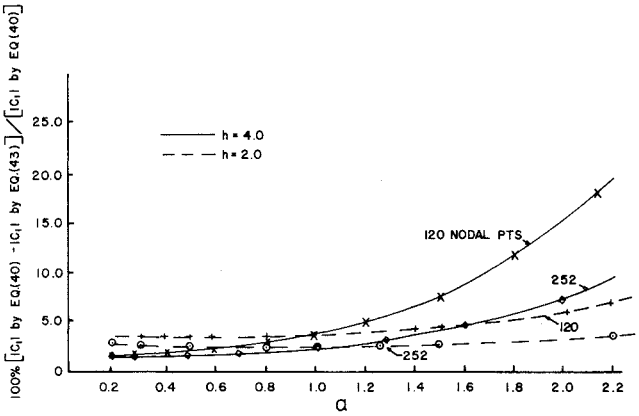

Fig. 5 Percent difference between Eq. (40) and Eq. (43) for a vertical circular cylinder.

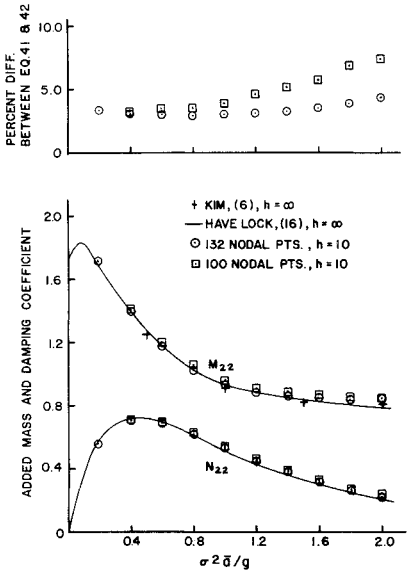

Fig. 6 Added mass and damping coefficients in heave for a floating hemisphere.

Fig. 5 wherein the results corresponding to $h = 2$ show only slight differences associated with the two subdivision numbers and both curves indicate only small error. The second configuration, $h = 4$ shows both a larger difference when compared to the closed form results in Fig. 4 as well as when compared with the results obtained using Eq. (43) as presented in Fig. 5. This apparently results from the fact that the $h = 4$ cylinder was generated by simply stretching the $h = 2$ cylinder and consequently the area elements are doubled in size and elongated.

The trend of the error plotted in Fig. 5 has been found to be typical of all numerical results regardless of body shape. The apparent reason for the increasing error with increasing frequency or decreasing wavelength is that the source potential, Eqs. (23) and (24), oscillates with increasing frequency as a increases. When the wavelength of this oscillation approaches the distance between nodal points, the accuracy of the numerical result is, of course, lost. Thus, if it were of interest to obtain results at high frequency, it would be necessary to use a fine subdivision grid. Fortunately, however, such results are generally of little practical importance.

The added mass and damping coefficients for a floating hemisphere corresponding to $h = 10$ for two different grid sizes are plotted in Fig. 6 along with the results of Havelock[16] and Kim[6] for $h = \infty$. The agreement appears to be satisfactory.

On the upper scale in Fig. 6 the percent difference obtained by use of Eqs. (41) and (42) is shown. As expected, the per cent difference is greater for the computations based on 100 nodal points as compared to the results based on 132 nodal points.

In Fig. 7 the horizontal and vertical component of the wave force acting on a floating hemisphere is plotted against the relative wavelength parameter, $a = 2\pi\bar{a}/\bar{L}$. Havelock's[16] results for the heave force for the infinite depth case is also plotted for comparison in Fig. 7, and the results agree well with the $h = 10$ case. [(Actually, Havelock did not calculate the force; the vertical force was calculated from his results for the damping coefficient by use of Eq. (45)].

The results for the wave forces shown in Fig. 7 are characterized by an increase in wave force with decreasing depth. At the short wave length end of the spectrum (large a) the forces always approach the deep water case. This results from the condition that if the waves are short, they are unaffected by the depth. That is, their effect does not reach to the bottom, and consequently, the water depth becomes unimportant.

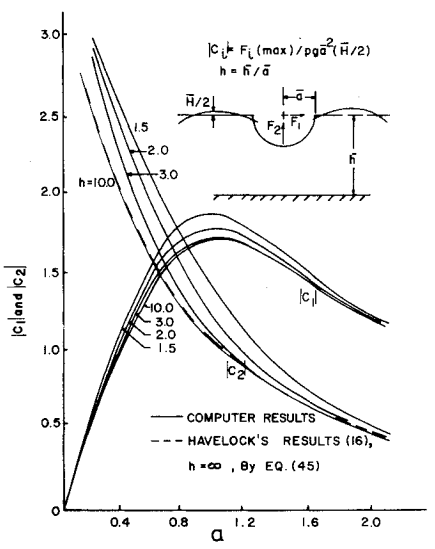

Fig. 7 Wave forces on a floating hemisphere.

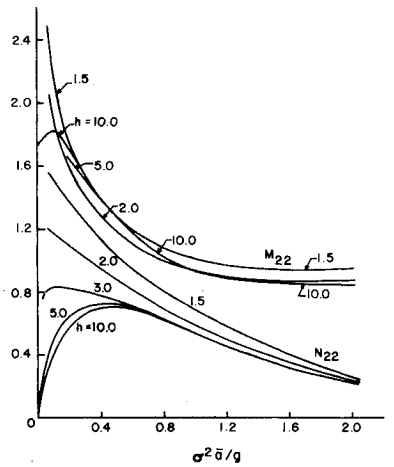

Fig. 8 Added mass and damping in heave for a floating hemisphere.

The added mass and damping coefficient in heave for a floating hemisphere is shown in Fig. 8 plotted against the frequency parameter, $\sigma^2\bar{a}/g$. The results are compared with the results of Havelock[16] for infinite depth. The figure shows generally that depth has a significant effect on the damping coefficient but affects the added mass coefficient to a lesser degree for this particular configuration.

The added mass and damping coefficient in surge for a floating hemisphere is shown in Fig. 9. The effect of depth on both coefficients appears to depend on the frequency. At low or zero frequency the effect of decreasing depth is shown to increase the added mass coefficient. At zero frequency the free surface appears as a rigid boundary and therefore the zero frequency case is equivalent to a sphere between parallel plates. Rigid boundary proximity always tends to increase the added mass.

Numerical Example

To demonstrate the capability of the method, wave forces and moment acting on a semisubmerged concrete caisson of practical shape, are calculated. The caisson used for example is shown in Fig. 10 having a rectangular base of 150 × 135 ft. in plan with a thickness of 25 ft. At each corner and as an integral part of the base, a 40 × 40 ft. column is formed which passes upward through the free surface. The corners of the columns are rounded with a radius of 4.0 ft.

Wave forces and the moment were calculated for the caisson sitting on the bottom for the following design condition with the wave propagation direction parallel to the

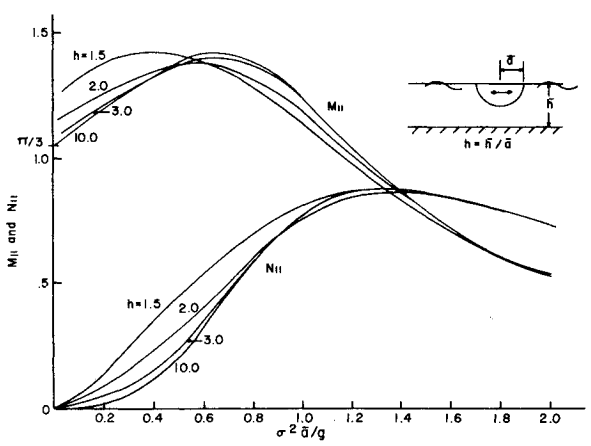

Fig. 9 Added mass and damping in surge for a floating hemisphere.

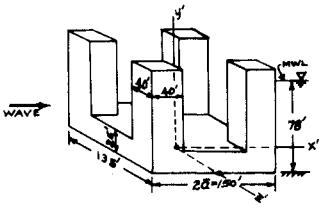

Fig. 10 Ocean caisson.

long side:

wave period	= 8.25 sec	a	= 1.48
water depth	= 78.0 ft	d	= 1.04
$\bar{a}$	= 75.0 ft	h	= 1.04

For these conditions the immersed surface of the caisson was partitioned into a total of 344 area elements for purposes of computer calculations.

The computed results based on the above conditions are:

force and moment coefficient	phase shift relative to wave crest
$\lvert C_1\rvert = 1.20$	$\delta_1 = -1.56$
$\lvert C_2\rvert = 1.38$	$\delta_2 = -2.38$
$\lvert C_6\rvert = 0.266$	$\delta_6 = 1.58$

The two components of force and the moment are given as:

horizontal force:	$F_1(t) = \rho g \bar{a}^3 \eta^\circ$	$\lvert C_1\rvert \cos(\delta_1 - \sigma t)$
vertical force:	$F_2(t) = \rho g \bar{a}^3 \eta^\circ$	$\lvert C_2\rvert \cos(\delta_2 - \sigma t)$
moment:	$F_6(t) = \rho g \bar{a}^4 \eta^\circ$	$\lvert C_6\rvert \cos(\delta_6 - \sigma t)$

One particular point of interest regarding these results is phase of the horizontal and vertical components of force. If the object is small in comparison to the wave length (small a), the horizontal force is maximum at $\sigma t = \pi/2$ and $3\pi/2$ and the maximum uplift force occurs at the trough where $\sigma t = \pi$. When a is not small, as in the present case, phase shifts occur. The results show the uplift force maximum to be shifted from the $\sigma t = \pi$ condition toward the maximum of the horizontal force. For a gravity structure this in-phase condition of the horizontal and uplift force represents a critical condition.

As a second example from practice, numerical results are presented for a typical North Sea structure in Fig. 11. The geometry represents the composite shape formed by two circular cylinders, one 400 ft and a second 100 ft in diameter. The large cylinder is 138 ft tall and has a flat top. In Fig. 10 the horizontal and vertical force and moment coefficients along with their phases are plotted as a function of wave periods in the range of practical interest.

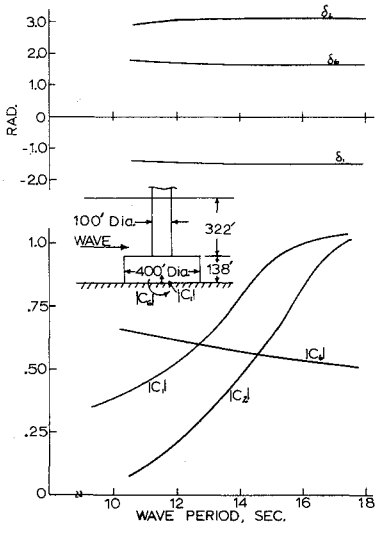

Fig. 11 Composite structure.

Conclusions

A practical numerical method has been developed utilizing digital computer calculations for the evaluation of hydrodynamic pressures, forces, and moments acting on rigid bodies. The results have been compared with analytical results for certain simple geometric configurations and the accuracy of the method shown to be typically within 5% but dependent on the frequency of the motion. Some results for a hemisphere oscillating at the free surface in water of finite depth have been presented, and a method for checking the accuracy of the numerical results proposed. Wave forces and moments were calculated for two different ocean structures.

References

[1]Sarpkaya, T. and Garrison, C. J., "Vortex Formation and Resistance in Unsteady Flow," *Journal of Applied Mechanics, Transactions of ASME,* Vol. 30, Series E, No. 1, March 1963, pp. 16–24.

[2]Keulegan, G. H. and Carpenter, L. H., "Forces on Cylinders and Plates in an Oscillating Fluid," *Journal of Research of the National Bureau of Standards,* Vol. 69, No. 5, May 1958, pp. 423–440.

[3]Dean, R. G. and Ursell, F., "Interaction of a Fixed, Semi-immersed Circular Cylinder with a Train of Surface Waves," Tech. Rept. 37, 1959, Hydrodynamics Lab MIT, Cambridge, Mass.

[4]Porter, W. R., "Pressure Distribution, Added-Mass and Damping Coefficients for Cylinders Oscillating in a Free Surface," Contract No. N-ONR-222(30), Series No. 82, Issue No. 16, July 1960 Institute of Engineering Research, University of Calif., Berkeley, Calif.

[5]Vugts, J. H., "The Hydrodynamic Coefficients for Swaying, Heaving and Rolling Cylinders in a Free Surface," *International Shipbuilding Progress,* Vol. 15, No. 167, July 1968, pp. 251–276.

[6]Kim, W. D., "On the Harmonic Oscillations of a Rigid Body on a Free Surface," *Journal of Fluid Mechanics,* Vol. 21, 1965, pp. 427–451.

[7]Garrison, C. J. and Seetharama Rao, V. "Interaction of Waves with Submerged Objects," *Journal of the Waterways, Harbors and Coastal Engineering Division, Proceedings of the ASCE,* Vol. 97, No. WW2, May 1971, pp. 259–277.

[8]Milgram, J. H. and Halkyard, J. E., "Wave Forces on Large Objects in the Sea," *Journal of Ship Research,* Vol. 15, No. 2, June 1971, pp. 115–124.

[9]Garrison, C. J. and Chow, P. Y., "Wave Forces on Submerged Bodies," *Journal of the Waterways, Harbors and Coastal Engineering Division, Proceedings of the ASCE,* Vol. 98, No. WW3, Aug 1972, pp. 375–392.

[10]Wehausen, J. V. and Laitone, E. V., "Surface Waves, Encyclopedia of Physics," *Fluid Dynamics III,* Vol. 9, edited by S. Flugge, Springer-Verlag, Berlin, 1960, p. 478.

[11]Monacella, V. J., "The Disturbance Due to a Slender Ship Oscillating in Waves in a Fluid of Finite Depth," *Journal of Ship Research,* Vol. 10, No. 4, 1966, pp. 242–252.

[12]Haskind, J. D., "The Exciting Forces and Wetting of Ships in Waves," (in Russian), *Isvestra Akademic Nauk SSSR, Otdelenie Teknicheskikh Nauk,* No. 7, 1957, pp. 65–78, (English translation available as David Taylor Model Basin Translation, No. 30, March 1962 Washington, D.C.

[13]Newman, J. N., "The Exciting Forces on Fixed Bodies in Waves," *Journal of Ship Research,* Vol. 6, 1962, pp. 10–17.

[14]Seetharama Rao, V., "Interaction of a Train of Regular Waves with a Rigid Submerged Ellipsoid," Ph.D. Dissertation, Dept. of Civil Engineering, Texas A&M University, College Station, Texas. May 1971, p. 157.

[15]MacCamy, R. C. and Fuchs, R. A., "Wave Forces on Piles: A. Diffraction Theory," Technical Memorandum 69, 1954, U.S. Army Corp of Engineers Beach Erosion Board, Washington, D.C.

[16]Havelock, T., "Waves Due to a Floating Sphere Making Periodic Heaving Oscillations," *Proceedings of the Royal Society,* Vol. 231, Series A, London, England, 1955, pp. 1–7.